Dynamic Surface Control for the Switched Reluctance Motor

1st Thuy Vo Thi Cam†
Electrical Department
Hanoi University of Industry
Hanoi, Viet Nam
vothuyhaui@gmail.com

2nd Dung Do Manh
Faculty of Applied Science
International School,VNU
Hanoi, Viet Nam
dungdm@vnuis.edu.vn

3rd Hai Le Xuan*
Faculty of Applied Science
International School,VNU
Hanoi, Viet Nam
hailx@vnu.edu.vn

4thKhoat Nguyen Duc
Faculty of Mechanical and Electrical
University of Mining and Geology
Hanoi, Viet Nam
nguyenduckhoat@humg.edu.vn

5th Minh Phan Xuan
Faculty of Applied Science
International School,VNU
Hanoi, Viet Nam
minh.phanxuan@hust.edu.vn

[1] ***Abstract*—The paper proposes a new method to improve the quality of the switching reluctance motor based on the dynamic surface control technique. The high-frequency noises generated by the switching process will be reduced by a low-pass filter. In addition, the derivative information collected directly from the controller also reduces the complexity of the controller implementation. The stability of the closed control system is ensured by a Lyapunov control function.**

***Index Terms*—Switched Reluctance Motor, Dynamic Surface Control, Backstepping method, the low-pass filter.**

I. Introduction

Switched Reluctance Motor (SRM) is a type of motor that has received a lot of attention in recent years because of its outstanding advantages - low manufacturing cost, high working temperature, and large torque, etc. Especially in the field of electric vehicle manufacturing, this type of engine is known as an integral component [1], [2], [3]. However, the switched reluctance motor still exists some disadvantages during operation including large pulse torque, noisy vibration, and difficulty to control. These disadvantages are the motivation for many papers to improve the control quality.

To overcome these above disadvantages, recent studies have focused on enhancing the control quality for SRM in two approaches: improving the accuracy in the SRM modeling process [4], [5] and applying suitable control algorithms for this object class [6], [7], [8], [9], [10]. The SRM mathematical model published by Rigatos et al [11] is quite advanced when the driver and the motor are integrated into the same mathematical model thereby increasing the accuracy of the SRM drivetrain.

In the work [11], Rigatos et al have linearized the SRM model to apply the linear control algorithm. On the basis of inheriting the nonlinear SRM mathematical model from [11], in this paper, the authors propose a DSC algorithm based on the Backstepping technique. The backstepping technique to control the speed stability for SRM has been studied by many works [12], [13], [14], [15]. However, this control technique is only applicable to the motor-specific SRM model. Theoretically, the Backstepping method can be applied to the general mathematical model of SRM in [11]. Nevertheless, the restriction lies in the Backstepping controller itself when the Backstepping control technique does not respond well to large noise. At the same time, SRM operates on the basis of switching and disconnecting the currents of the phases, so that vibration and harmonics exist at high switching frequencies [16], [17], [18], [19]. These high-frequency harmonics degrade the performance of the control scheme, and in many awful cases, they can make the closed-loop system to be unstable. To improve the robustness of the closed-loop scheme when confronting the lumped disturbances, the sliding mode controller [9], [10] is a popular controller but this method causes the chattering phenomenon in the response of the system's outputs. This is bad for the engine.

Therefore, an idea about integrating a low pass filter into the Backstepping controller naturally arises to solve this problem since the low pass filter (LPF) not only can be eliminated the high-frequency disturbances but also estimated LPF's input signal by only adjusting its time parameter. The Backstepping controller with a low pass filter to estimate the virtual control is called Dynamic Surface Controller (DSC). The DSC method based on the Backstepping perspectives is first designed in this paper for the nonlinear SRM system with mismatched disturbances and high-frequency harmonic from the switching process to steer its angular velocity to track the desired value. The stability of the closed-loop system is systematically proven by the Lyapunov theorem. All results are simulated in the Matlab-Simulink platform, and the control performance under the influence of the DSC controller is compared to itself when utilizing the classical Backstepping method simultaneously.

The remaining part of this paper is: Section 2 presents the

[1]†: Faculty of Mechanical and Electrical, University of Mining and Geology, Hanoi, Vietnam
*: Corresponding author's email address: hailx@vnu.edu.vn

foundational knowledge which is necessary to design the DSC controller for the SRM system successfully. It consists of the DSC technique and the mathematical model of the SRM. The detailed design procedure of the DSC controller for the SRM system is presented in Section 3. All the results, as well as the effectiveness of the DSC controller, are demonstrated in Section 4. Conclusions are presented in the final section.

In this paper, $\underline{x}$ is symbolized for the column vector of $n > 0$ real numbers $x_1, x_2, ..., x_n$. $\dot{\underline{x}}$ presents the first-order derivation of vector $\underline{x}$. $\|\underline{x}\|$ is the 2-norm of vector $\underline{x}$ which is calculated by $\|\underline{x}\| = \|\underline{x}\|_2 = \sqrt{\sum_{i=1}^{n} x_i^2}$. $\mathbb{R}^{n\times m}$ presents the space of $n \times m$ matrices and $\mathbb{R}^n$ is the short presenting of $\mathbb{R}^{n\times 1}$. G^T is a transpose matrix of a matrix G and t_o is symbolized for the initial time.

II. The foundational knowledge

A. Dynamic surface control technique for second-order back-propagation system

Consider the second-order nonlinear system

$$\begin{cases} \dot{\underline{z}}_1 = \underline{z}_2 + \underline{d}(\underline{z}_1, \underline{z}_2, t) \\ \dot{\underline{z}}_2 = \underline{f}(\underline{z}_1, \underline{z}_2) + G(\underline{z}_1, \underline{z}_2)\underline{u} \end{cases} \tag{1}$$

Where $\underline{z}_1 \in \mathbb{R}^n$ is the state vector of the nonlinear system (1), $\underline{z}_2 \in \mathbb{R}^n$, $\underline{u} \in \mathbb{R}^p$ is the vector of p input signals, $\underline{f}(\underline{z}_1, \underline{z}_2)$ is a nonlinear continuous functions vector and $G(\underline{z}_1, \underline{z}_2) \in \mathbb{R}^{n\times m}$ is a nonlinear continuous functions matrix with the assumption that $G(\underline{z}_1, \underline{z}_2)$ is full-rank. $\underline{d}(\underline{z}_1, \underline{z}_2, t) \in \mathbb{R}^n$ is the vector of time-varying mismatched disturbances. In this paper, $\underline{d}(\underline{z}_1, \underline{z}_2, t)$ is an unknown vector, and assumed that $\underline{d}(\underline{z}_1, \underline{z}_2, t)$ and all system's states are bounded.

The control objective for system (1) is to force the state variable to track the reference. To make this happen, contain two steps, the dynamic surface control technique for (1) can be described as follow:

Step 1: Define the tracking error as well as the first sliding surface by

$$\underline{\varepsilon}_1 = \underline{z}_1 - \underline{z}_d \tag{2}$$

Taking the derivative of $\underline{\varepsilon}_1$ we have

$$\dot{\underline{\varepsilon}}_1 = \dot{\underline{z}}_1 - \dot{\underline{z}}_d = \underline{z}_2 - \dot{\underline{z}}_d + \underline{d}(\underline{z}_1, \underline{z}_2, t) \tag{3}$$

The second sliding surface designed according to the Back-stepping technique is defined as:

$$\underline{\varepsilon}_2 = \underline{z}_2 - \underline{\alpha}_1 \tag{4}$$

with $\underline{\alpha}_1$ is the virtual control signal. From these equations (3) and (4) we have:

$$\dot{\underline{\varepsilon}}_1 = \underline{\varepsilon}_2 + \underline{\alpha}_1 - \dot{\underline{z}}_d + \underline{d}(\underline{z}_1, \underline{z}_2, t) \tag{5}$$

and the virtual control signal $\underline{\alpha}_1$ is determined to stabilize the first sliding surface according to [21]:

$$\underline{\alpha}_1 = -c_1\underline{\varepsilon}_1 + \dot{\underline{z}}_d - \underline{d}(\underline{z}_1, \underline{z}_2, t) \tag{6}$$

Where $c_1 > 0$ is a positive constant.

Step 2: From equation (4), differentiating $\underline{\varepsilon}_2$ over time gives:

$$\dot{\underline{\varepsilon}}_2 = \dot{\underline{z}}_2 - \dot{\underline{\alpha}}_1 = \underline{f}(\underline{z}_1, \underline{z}_2) + G(\underline{z}_1, \underline{z}_2)\,\underline{u} - \dot{\underline{\alpha}}_1 \tag{7}$$

Since the matrix $G(\underline{z}_1, \underline{z}_2)$ is a full-rank matrix, there always exists a pseudo-inverse matrix $G^*(\underline{z}_1, \underline{z}_2)$ which is calculated by $G^*(\underline{z}_1, \underline{z}_2) = G^T(\underline{z}_1, \underline{z}_2)\left[G(\underline{z}_1, \underline{z}_2)\,G^T(\underline{z}_1, \underline{z}_2)\right]^{-1}$. The control signal of DSC is calculated as

$$\underline{u} = G^*(\underline{z}_1, \underline{z}_2)\left[-c_2\underline{\varepsilon}_2 - \underline{\varepsilon}_1 - \left(\underline{f}(\underline{z}_1, \underline{z}_2) - \dot{\underline{\alpha}}_1\right)\right] \tag{8}$$

Where $c_2 > 0$ is a positive constant chosen arbitrarily. Substituting the equation (4) into equation (8) gives:

$$\underline{u} = G^*(\underline{z}_1, \underline{z}_2)\left[-c_2\underline{z}_2 - \underline{\varepsilon}_1 - \underline{f}(\underline{z}_1, \underline{z}_2) + \dot{\underline{\alpha}}_1 + c_2\underline{\alpha}_1\right] \tag{9}$$

As can be seen from equation (9), it must determine $\underline{\alpha}_1$ exactly to handle the control input $\underline{u}$. However, due to the unknown disturbance vector $\underline{d}(\underline{z}_1, \underline{z}_2, t)$, measuring $\underline{\alpha}_1$ can lead to confronting various challenging. Therefore, a low pass filter (LPF) is proposed for estimating the virtual control signal and its first-order derivation as the following equation:

$$\begin{cases} \hat{\underline{d}}(\underline{z}_1, \underline{z}_2, t) = \hat{\dot{\underline{z}}}_1 - \underline{z}_2 \\ \hat{\underline{\alpha}}_1 = -c_1\underline{\varepsilon}_1 + \dot{\underline{z}}_d - \hat{\underline{d}}(\underline{z}_1, \underline{z}_2, t) \\ \tau_f\dot{\underline{\alpha}}_{1f} + \underline{\alpha}_{1f} = \hat{\underline{\alpha}}_1 \\ \underline{\alpha}_{1f}(t_o) = \hat{\underline{\alpha}}_1(t_o) \end{cases} \tag{10}$$

Where $\hat{\dot{\underline{z}}}_1 \approx \frac{\underline{z}_1(t) - \underline{z}_1(t-T_s)}{T_s}$ is the approximation of the first-order of $\underline{z}_1$ by applying the backward differentiating formula. T_s is the time parameter that is chosen small arbitrarily. $\hat{\underline{d}}(\underline{z}_1, \underline{z}_2, t)$ and $\hat{\underline{\alpha}}_1$ are the estimation of $\underline{d}(\underline{z}_1, \underline{z}_2, t)$, $\underline{\alpha}_1$, respectively. τ_f is the time parameter of LPF. The LPF is considered a linear system in which the vector of its states is $\underline{\alpha}_{1f}$. $\underline{\alpha}_{1f}(t_o)$ and $\hat{\underline{\alpha}}_1(t_o)$ are $\underline{\alpha}_{1f}$, $\hat{\underline{\alpha}}_1$ at the initial time, respectively.

It can be seen that if τ_f is chosen sufficiently small, $\underline{\alpha}_{1f}$ will approximate $\underline{\alpha}_1$ leading to:

$$\underline{\alpha}_1 \approx \hat{\underline{\alpha}}_1 \approx \underline{\alpha}_{1f} \Rightarrow \dot{\underline{\alpha}}_1 \approx \hat{\dot{\underline{\alpha}}}_1 \approx \dot{\underline{\alpha}}_{1f} = \frac{\hat{\underline{\alpha}}_1 - \underline{\alpha}_{1f}}{\tau_f} \tag{11}$$

And $\dot{\underline{\alpha}}_{1f}$ will be utilized instead of $\dot{\underline{\alpha}}_1$ to design the control signal in the following step.

Step 3: From these equations (10) and (11), the vector of input signals is determined by:

$$\underline{u} = G^*(\underline{z}_1, \underline{z}_2)\left[-c_2\underline{z}_2 - \underline{\varepsilon}_1 - \underline{f}(\underline{z}_1, \underline{z}_2) + \dot{\underline{\alpha}}_{1f} + c_2\hat{\underline{\alpha}}_1\right] \tag{12}$$

Remark 1: *The backstepping method cannot design for the nonlinear system with mismatched disturbances. Therefore, the DSC method is more general than the one.*

Remark 2: *Different from the backstepping controller [21], by adding an LPF behind the virtual control signal, the dynamic surface controller not only can estimate the virtual control signal but also can eliminate the "explosion of terms" phenomenon caused by the switching process, as well as the*

influence of the high-frequency disturbances. Thus, the DSC method is obviously more effective than using the disturbance observer such as in the work [23].

B. The mathematical model of the SRM system

This section briefly presents the constructing process of the mathematical model of m-phase SRMs that was studied in [11] from three main equations: armature voltage equation, electro-magnetic equation, and mechanical equation (13):

$$\begin{cases} u_j = Ri_j + \dfrac{d\psi_j}{dt} \\ T_j(\theta, i_j) = \dfrac{\partial W_j^{'}}{\partial \theta} \\ J\dfrac{d^2\theta}{dt^2} = T_e - T_l \end{cases} \tag{13}$$

Where $j = 1, 2, ..., m$. The notations u_j, R, i_j, ψ_j are the voltage, resistor, current, and flux of j^{th} phase, respectively. T_e is the torque of phase, T_l is the torque of load, J is the moment of inertia and $W_j^{'}$ is the electro-magnetic energy calculated by:

$$\partial \mathrm{W}_j^{'}(\theta, i_j) = \int_0^{i_j} \psi_j(\theta, i_j) di_j \tag{14}$$

The total torque of phase T_e is determined by taking the sum of moments in each phase

$$T_e(\theta, i_1, i_2, ..., i_m) = \sum_{j=1}^{m} T_j(\theta, i_j) \tag{15}$$

The function of magnetic flux characteristic can be approximated by [11]:

$$\psi_j(\theta, i_j) = \psi_s(1 - e^{-i_j f_j(\theta)}) \tag{16}$$

In which ψ_s is the saturation flux and $f_j(\theta)$ is estimated by Fourier series with N_r is number of rotor's pole

$$f_j(\theta) = a + b\sin\left[N_r\theta - (j-1)\frac{2\pi}{m}\right] \tag{17}$$

The torque of phase j is represented as follows:

$$T_j(\theta, i_j) = \frac{\psi_s}{f_j^2(\theta)} \frac{df_j(\theta)}{d\theta} \left\{1 - [1 + i_j f_j(\theta)]\, e^{-i_j f_j(\theta)}\right\} \tag{18}$$

In this paper, the SRM with 4-phase will be considered so that $m = 4$ and the state vector is defined as follow: $\underline{x} = [\theta, \omega, i_1, i_2, i_3, i_4]^T = [x_1, x_2, x_3, x_4, x_5, x_6]^T$. The state-space equations of the motor can be rewritten as:

$$\begin{cases} \dot{x}_1 = x_2 \\ \dot{x}_2 = [f_a(\underline{x}) + g_a(\underline{x})x_3] + [f_b(\underline{x}) + g_b(\underline{x})x_4] \\ \qquad + [f_c(\underline{x}) + g_c(\underline{x})x_5] + [f_c(\underline{x}) + g_c(\underline{x})x_6] \\ \qquad - \dfrac{B}{J}x_2 + \dfrac{mgl}{J}\sin x_1 \\ \dot{x}_3 = p_a(\underline{x}) + q_a(\underline{x})u_1 \\ \dot{x}_4 = p_b(\underline{x}) + q_b(\underline{x})u_2 \\ \dot{x}_5 = p_c(\underline{x}) + q_c(\underline{x})u_3 \\ \dot{x}_6 = p_d(\underline{x}) + q_d(\underline{x})u_4 \end{cases} \tag{19}$$

Where $f_i(\underline{x})$, $g_i(\underline{x})$, $p_i(\underline{x})$ and $q_i(\underline{x})$ are calculated in [11] with $i = a, b, c, d$.

III. Design the DSC controller for SRM system and analysis of the control performance

A. Design the DSC controller for SRM system

Step 1: *Converting the mathematical of the SRM system*
It is necessary to convert the SRM's mathematical model to the form to be applied to the DSC algorithm. Taking the derivative of the second equation of (19) we have:

$$\begin{aligned} \ddot{x}_2 = &\left[\dot{f}_a(\underline{x}) + \dot{g}_a(\underline{x})x_3 + g_a(\underline{x})p_a(\underline{x}) + g_a(\underline{x})q_a(\underline{x})u_1\right] \\ &+ \left[\dot{f}_b(\underline{x}) + \dot{g}_b(\underline{x})x_4 + g_b(\underline{x})p_b(\underline{x}) + g_b(\underline{x})q_b(\underline{x})u_2\right] \\ &+ \left[\dot{f}_c(\underline{x}) + \dot{g}_c(\underline{x})x_5 + g_c(\underline{x})p_c(\underline{x}) + g_c(\underline{x})q_c(\underline{x})u_3\right] \\ &+ \left[\dot{f}_d(\underline{x}) + \dot{g}_d(\underline{x})x_6 + g_d(\underline{x})p_d(\underline{x}) + g_d(\underline{x})q_d(\underline{x})u_4\right] \\ &- \frac{B}{J}\dot{x}_2 + \frac{mgl}{J}\cos x_1\dot{x}_1 \end{aligned} \tag{20}$$

The switched reluctance motor works with the principle of voltage supply for each phase so if $m = 4$, we have $u_j = k_j u$ where k_j is phase transition key that can only take 2 values, 0 or 1, and if we denote

$$\begin{aligned} f(\underline{x}) = &\dot{f}_a(\underline{x}) + \dot{g}_a(\underline{x})x_3 + g_a(\underline{x})p_a(\underline{x}) \\ &+ \dot{f}_b(\underline{x}) + \dot{g}_b(\underline{x})x_4 + g_b(\underline{x})p_b(\underline{x}) \\ &+ \dot{f}_c(\underline{x}) + \dot{g}_c(\underline{x})x_5 + g_c(\underline{x})p_c(\underline{x}) \\ &+ \dot{f}_d(\underline{x}) + \dot{g}_d(\underline{x})x_6 + g_d(\underline{x})p_d(\underline{x}) \end{aligned} \tag{21}$$

and

$$\begin{aligned} g(\underline{x}) = &g_a(\underline{x})q_a(\underline{x})k_1 + g_b(\underline{x})q_b(\underline{x})k_2 \\ &+ g_c(\underline{x})q_c(\underline{x})k_3 + g_d(\underline{x})q_d(\underline{x})k_4 \end{aligned} \tag{22}$$

The equation (20) can be rewritten as

$$\ddot{x}_2 + \frac{mgl}{J}\cos(x_1)\dot{x}_1 + \frac{B}{J}\dot{x}_2 = f(\underline{x}) + g(\underline{x})u \tag{23}$$

and we obtain the velocity mathematic model of the SRM.

Step 2: *Design the DSC controller for SRM system*

Designing the DSC controller for the SRM system, from (23), let us define $x_2 = z_1$, we have the second-order backpropagation model of the SRM's velocity given by

$$\begin{cases} \dot{z}_1 = z_2 - m(x_1, x_2) \\ \dot{z}_2 = f(z_1, z_2) + g(z_1, z_2)\, u \end{cases} \tag{24}$$

Where

$$m(x_1, x_2) = \frac{mgl}{J} \int_0^t cos(x_1(\tau)) \dot{x_1}(\tau) d(\tau) + \frac{B}{J} x_2 \tag{25}$$

These functions $f(z_1, z_2) = f(\underline{x})$ and $g(z_1, z_2) = g(\underline{x})$ are calculated by (21), (22). By defining $\varepsilon_1 = z_1 - z_{1d}$, which is the tracking error between z_1 and its desired signal z_{1d}, we also have:

$$\begin{cases} \dot{\varepsilon}_1 = z_2 - d(x_1, x_2, t) \\ \dot{z}_2 = f(z_1, z_2) + g(z_1, z_2)\, u \end{cases} \tag{26}$$

Where $d(x_1, x_2, t) = m(x_1, x_2) + \dot{z}_{1d}$ is the vector of all time-varying lumped disturbances. Note that $g^*(x_1, x_2) = g^{-1}(x_1, x_2)$ due to the scalar continuous function $g(x_1, x_2)$. The dynamic surface control signal is determined by (12)

$$u = \frac{-c_2 z_2 - \varepsilon_1 - f(z_1, z_2) + \dot{\alpha}_{1f} + c_2 \hat{\alpha}_1}{g(z_1, z_2)} \tag{27}$$

B. Analysis of the control performance

Theorem 1: *The dynamic surface controller (27) will make the tracking error of system (26) bounded by a neighborhood of zero.*

Proof: The Lyapunov function is chosen for closed loop system has the following form

$$V_{dsc} = \frac{1}{2}\varepsilon_1^2 + \frac{1}{2}\varepsilon_2^2 + \frac{1}{2}\varepsilon_f^2 \tag{28}$$

Differentiating V_{dsc} over time, and using equations (3) and (12), we have:

$$\begin{aligned} \dot{V}_{dsc} &= \varepsilon_1 \dot{\varepsilon}_1 + \varepsilon_2 \dot{\varepsilon}_2 + \varepsilon_f \dot{\varepsilon}_f \\ &= \varepsilon_1 (-c_1 \varepsilon_1 + \varepsilon_2 + \varepsilon_f) + \varepsilon_2 (-\varepsilon_1 - c_2 \varepsilon_2 + \varepsilon_f) + \varepsilon_f \dot{\varepsilon}_f \\ &= -c_1 \varepsilon_1^2 - c_2 \varepsilon_2^2 + \varepsilon_1 \varepsilon_f + \varepsilon_f \dot{\varepsilon}_f + \varepsilon_2 \varepsilon_f \end{aligned} \tag{29}$$

Where $\varepsilon_f = \alpha_{1f} - \hat{\alpha}_1$ we obtain:

$$\dot{\varepsilon}_f = \dot{\alpha}_{1f} - \dot{\hat{\alpha}}_1 = -\frac{1}{\tau_f}\varepsilon_f + c_1 \dot{\varepsilon}_1 - \ddot{z}_d + \dot{\hat{d}}(x_1, x_2, t) \tag{30}$$

Due to the bounded conditions of the SRM's states, the first order derivative of velocity tracking error $\dot{\varepsilon}_1$ and the second order derivative of desire trajectory velocity $\ddot{z}_d$, it can be presented that:

$$\left\| c_1 \dot{\varepsilon}_1 - \ddot{z}_d + \dot{\hat{d}}(x_1, x_2, t) \right\| < \beta \tag{31}$$

with β is a positive constant. From (29), (30) and (31) we have:

$$\dot{V}_{dsc} < -c_1 \varepsilon_1^2 - c_2 \varepsilon_2^2 + \varepsilon_1 \varepsilon_f + \varepsilon_2 \varepsilon_f - \frac{1}{\tau_f}\varepsilon_f^2 + \|\varepsilon_f \beta\| \tag{32}$$

Using Cauchy inequality as

$$\varepsilon_{1,2}\varepsilon_f \le \varepsilon_{1,2}^2 + \frac{1}{4}\varepsilon_f^2, \ \|\varepsilon_f \beta\| \le \frac{\varepsilon_f^2 \beta^2}{4\xi} + \xi \tag{33}$$

Where ξ is an arbitrarily small positive constant. Substituting (32) into (33) leading to

$$\dot{V}_{dsc} < -(c_1 - 1)\varepsilon_1^2 - (c_2 - 1)\varepsilon_2^2 - \left(\frac{1}{\tau_f} - \frac{1}{4} - \frac{\beta^2}{4\xi}\right)\varepsilon_f^2 + \xi \tag{34}$$

The parameters c_1, c_2 and τ_f are now designed as:

$$c_1 \ge 1 + \frac{c}{2}, \ c_2 \ge 1 + \frac{c}{2}, \ \tau_f \le \frac{4\xi}{2c\xi + \xi + \beta^2} \tag{35}$$

with c is a positive constant, the inequation (34) become:

$$\dot{V}_{dsc} < -c\left(\frac{1}{2}\varepsilon_1^2 + \frac{1}{2}\varepsilon_2^2 + \frac{1}{2}\varepsilon_f^2\right) + \xi = -cV_{dsc} + \xi \tag{36}$$

It can be seen that when $-cV_{dsc} + \xi \ge 0$ or $V_{dsc} \le \xi/c$ we small positive constant, the velocity tracking error ε_1 will be bounded in an arbitrarily small neighborhood of zero. On the other hand, if $-cV_{dsc} + \xi < 0$ we also have $\dot{V}_{dsc} < 0$ thereby making the velocity tracking error ε_1 converged to a neighborhood of zero according to Lyapunov's criterion. Thus, the proof is completed.

IV. Numerical simulation and discussion

The effectiveness of the proposed control strategy will be verified through the simulation process on Matlab/Simulink and compared with the Backstepping method. First, the parameters of the SRM and the DSC controller are presented in Table. 1. Then, two scenarios of simulation are undertaken to evaluate the performance of LPF as well as the DSC controller in which the time parameter τ_f of LPF is considered between 3 values 0.01s, 0.1s, and 0.2s. In addition, the Backstrpping method designed in two scenarios is handled with the assumption that the mismatched disturbance vector $d(x_1, x_2, t)$ is equal to zero.

TABLE I
Parameters of the SRM and the DSC controllers

$J = 9.68.10^3 (kg/m^2)$	$B = 0.2$	$l = 2(m)$
$\alpha = 1.5.10^{-3}(H)$	$R = 0.05(\Omega)$	$c_1 = 1$
$b = 1.364.10^{-3}(H)$	$T = 0.025$	$c_2 = 3$

Scenario 1: *The system is not affected by the disturbances and the reference is a fixed set point at 10 rad/s.*

It can be observed in **Scenario 1** that when the SRM is not affected by the disturbances, both the virtual control signal and its derivation can be effectively approximated by LPF, which leads to the control quality of SRM's velocity in the case of using a dynamic surface controller is not inferior to that of using a backstepping controller. Furthermore, in Figure (1) we can also see that the settling time when using DSC is smaller than using the backstepping controller. The influence of the time parameter on the approximation task is shown in Figure

(2) and Figure (3), we can observe that the red line is closest to the black line which presents the virtual control signal and its derivation of the backstepping controller. This result affirms that the smaller the time parameter, the better the approximation quality of LPF. Besides, the stability of the closed-loop system does not depend on the time parameter τ_f of the low-pass filter. For this scenario, the Dynamic Surface Control method is demonstrated its effectiveness which brings to the control performance. Additionally, the ability to eliminate the high-frequency noise depending on the filter parameter will be more clearly demonstrated in **Scenario 2**.

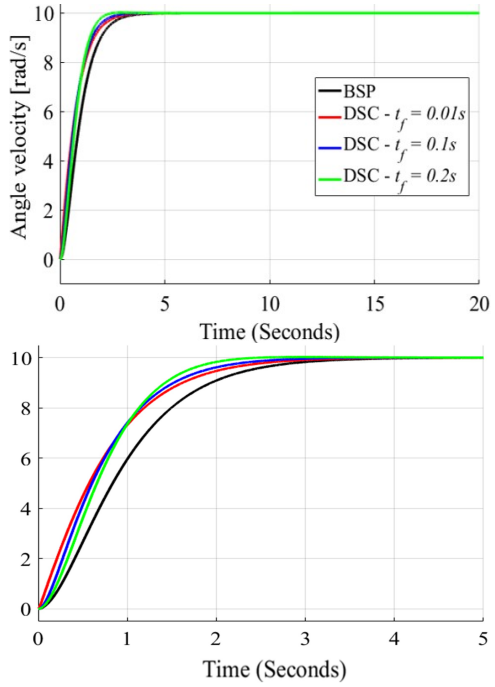

Fig. 1. The response of the angular velocity within 20 seconds and 5 seconds

Scenario 2: *When there exist high-frequency disturbances (see Figure (4)) that affect the virtual control signal α_1. The reference is still kept at 10 rad/s*

Different from the first scenario, scenario 2 focuses on the advantage of LPF in minimizing the effects of high-frequency disturbance on SRM. Figure. 6 and Figure. 7 shows that after going through LPF the magnitude of disturbances as well as the influence of high-frequency components have been reduced and the bigger the time parameter τ_f, the better the filter performance. LPF in this case unfortunately no longer retains good approximation quality, however, the limitation of the high-frequency terms in disturbances gives a better control quality which can be observed in Figure 5. Thereby, even if there are errors in the approximation process of α_1 and $\dot{\alpha}_1$, the dynamic surface controller can still steer the velocity of SRV to the desired velocity, which had been acknowledged in **Theorem 1**.

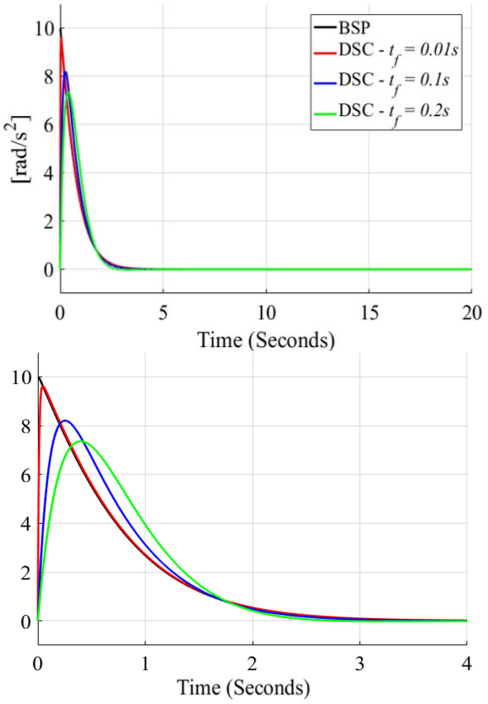

Fig. 2. The response of the virtual control α_1 within 20 seconds and 4 seconds

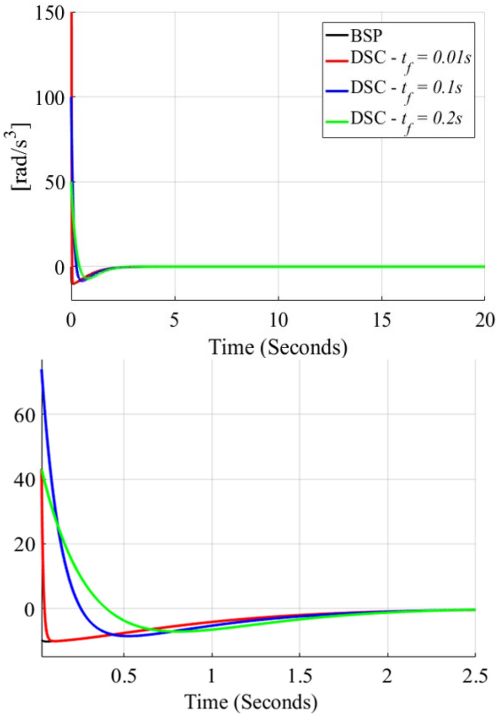

Fig. 3. The response of the derivation of the virtual control $\dot{\alpha}_1$ within 20 seconds and 2.5 seconds

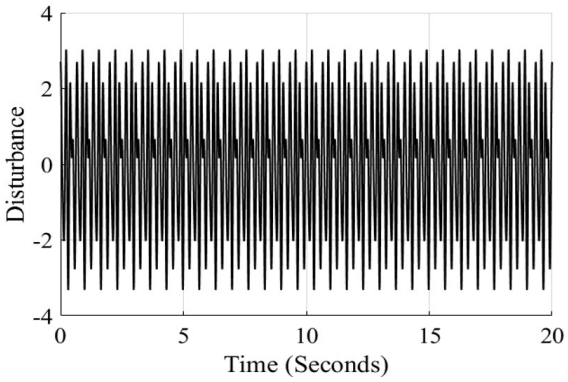

Fig. 4. The high-frequency disturbance

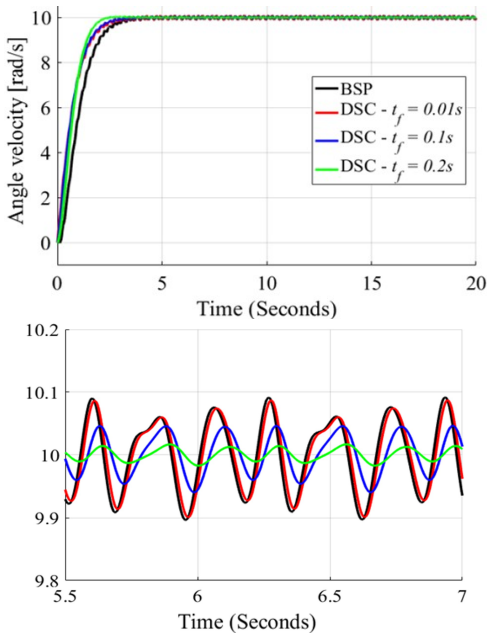

Fig. 5. The response of the SRM's angular velocity within 20 seconds and 7 seconds

Through two simulation scenarios, we can conclude that the control performance when applying the Dynamic Surface Control method is equivalent to doing so when utilizing the Backstepping algorithm in the ideal scenario without the environmental disturbances. In the case of the influence of high-frequency unpredictable disturbances, the DSC controller becomes more optimal with a smaller error amplitude. The reason why the DSC controller is so superior is that its construct-in low-pass filters are capable of preserving the DC component of the signals.

V. Conclusion

In this paper, we applied dynamic surface control (DSC) to stabilize the angular velocity of the switched reluctance motor at the desired value. The results were simulated by the Matlab-Simulink platform, and they were compared with the simulation results by utilizing the Backstepping method. In general, the output responses with the DSC method are

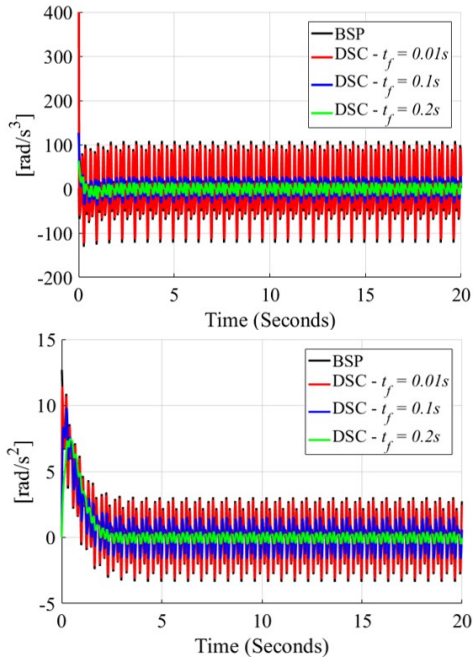

Fig. 6. The approximation results of α_1 and $\dot{\alpha}_1$ within 20 seconds

better than itself when applying the Backstepping algorithm. In addition, due to the integration of the low-pass filter with a suitable frequency parameter in the DSC design procedure, most high-order harmonic are eliminated. It leads to the fact that the estimated results by the DSC method when the influence of the high-order disturbances is always in the system are better than by using the Backstepping method.

References

[1] Diego F.Valencia, Rasul Tarvirdilu-Asl, Cristian Garcia, Jose Rodriguez, Ali Emadi, "Vision, Challenges, and Future trends of model predictive control in switched reluctance motor drives", *IEEE*, vol. 9, 2021, pp. 69926-69937.

[2] J.-W. Ahn and G. F. Lukman, "Switched reluctance motor: Research trends and overview", *CES Trans. Electr. Mach. Syst.*, vol. 2, no. 4, 2018, pp. 339–347.

[3] B. Bilgin, B. Howey, A. D. Callegaro, J. Liang, M. Kordic, J. Taylor, and A. Emadi, "Making the case for switched reluctance motors for propulsion applications", *IEEE Trans. Veh. Technol.*, vol. 69, no. 7, 2020, pp. 7172–7186.

[4] J. A. Makwana, P. Agarwal, and S. P. Srivastava. - Modeling and Simulation of Switched Reluctance Motor, Lect. Notes Electr. Eng. 442 (2018) 545–558.

[5] A. Nirgude, M. Murali, N. Chaithanya, S. Kulkarni, V. B. Bhole, and S. R. Patel, "Nonlinear mathematical modeling and simulation of switched reluctance motor", IEEE Int. Conf. Power Electron. Drives Energy Syst. PEDES 2016. vol. 2016, January, (2017) 1–6. Doi: 10.1109/PEDES.2016.7914462.

[6] K. F. Wong, K. W. E. Cheng, and S. L. Ho (2009), "On-line instantaneous torque control of a switched reluctance motor based on co-energy control", IET Electr. Power Appl., vol. 3, no. 4, pp. 257–264.

[7] Arun Chithrabhanu, Krishna Vasudevan (2021), "Current Sharing Function Based Torque Ripple Reduction Strategy For Switched Reluctance Motor Drives", 2021 IEEE 12th Energy Conversion Congress and Expostive Asia.

[8] C. Labiod, K. Srairi, B. Mahdad, M. T. Benchouia, and M. E. H. Benbouzid (2015), "Speed Control of 8/6 Switched Reluctance Motor with Torque Ripple Reduction Taking into Account Magnetic Saturation Effects", Energy Procedia, vol. 74, pp. 112–121.

[9] M. Rafiq, S. U. Rehman, F. U. Rehman, Q. R. Butt, and I. Awan (2012), "A second order sliding mode control design of a switched reluctance motor using super twisting algorithm", Simul. Model. Pract. Theory, vol. 25, pp. 106–117.

[10] J. Sun, G. Z. Cao, S. D. Huang, Y. Peng, J. He, and Q. Q. Qian (2019), "Sliding-Mode-Observer-Based Position Estimation for Sensorless Control of the Planar Switched Reluctance Motor", IEEE Access, vol. 7, pp. 61034–61045.

[11] G. Rigatos, P. Siano, and S. Ademi. - Nonlinear H-infinity control for switched reluctance machines, Nonlinear Eng. 9 (1) (2019) 14–27. Doi:10.1515/nleng-2017-0114.

[12] J. J. Carroll, A. J. Geoghan, D. M. Dawson, and P. Vedagarbha (1995), "Backstepping based computed torque controller for switched reluctance motors driving inertial loads", IEEE Conf. Control Appl. - Proc., pp. 779–786.

[13] C. H. Lin (2019), "Adaptive nonlinear backstepping control using mended recurrent Romanovski polynomials neural network and mended particle swarm optimization for switched reluctance motor drive system", Trans. Inst. Meas. Control, vol. 41, no. 14, pp. 4114–4128.

[14] M. T. Alrifai, J. H. Chow, and D. A. Torrey (2000), "Practical application of backstepping nonlinear current control to a switched-reluctance motor", Proc. Am. Control Conf., vol. 1, no. June, pp. 594–599

[15] Lin, C. H. (2019). Adaptive nonlinear backstepping control using mended recurrent Romanovski polynomials neural network and mended particle swarm optimization for switched reluctance motor drive system. Trans. Inst. Meas. Control, 41 (14), 4114-4128.

[16] Charles Pollock, Chi Yao Wu, "Acoustic Noise Cancellation Techniques for Switched Reluctance Drives", IEEE, vol. 33, no. 2, pp. 477 – 484, 1997.

[17] Roy S. Colby, Francois M. Mottier, J. E. Miller, "Vibration Modes and Acoustic Noise in a Four-Phase Switched Reluctance Motor", IEEE, vol. 32, no. 6, pp. 1357 – 1364, 1996.

[18] Wei Cai, Pragasen Pillay, Zhangjun Tang, "Impact of Stator Windings and End-Bells on Resonant Frequencies and Mode Shapes of Switched Reluctance Motors", IEEE, vol. 38, no. 4, pp. 1027 – 1036, 2002.

[19] Jian Li, Yunhyun Cho, "Investigation into Reduction of Vibration and Acoustic Noise in Switched Reluctance Motors in Radial Force Excitation and Frame Transfer Function Aspects", IEEE, vol. 45, no. 10, pp. 4664 – 4667, 2009.

[20] H. Magsi, A. H. Sodhro, F. A. Chachar and S. A. K. Abro, "Analysis of signal noise reduction by using filters", 2018 Int. Conf. Comput. Math. Eng. Technol. Inven. Innov. Integr. Socioecon. Dev. iCoMET 2018 - Proc., vol. 2018-Janua, pp. 1-6, 2018.

[21] Jing Zhou and Changyun Wen, *Adaptive Backstepping Control of Uncertain Systems: Nonsmooth Nonlinearities, Interactions or Time-Variations*, Lecture Notes in Control and Information Sciences, Springer, 2008.

[22] Bongsob Song and J. Karl Hedrick, *Dynamic Surface Control of Uncertain Nonlinear Systems, An LMI Approach*, Springer, 2011

[23] Q. D. Nguyen et al., "Robust Sliding Mode Control-Based a Novel Super-Twisting Disturbance Observer and Fixed-Time State Observer for Slotless-Self Bearing Motor System," in IEEE Access, vol. 10, pp. 23980-23994, 2022, doi: 10.1109/ACCESS.2022.3155121.